

# CMLCompiler: A Unified Compiler for Classical Machine Learning

Xu Wen

Institute of Computing Technology,  
Chinese Academy of Sciences  
University of Chinese Academy of  
Sciences  
wenxu@ict.ac.cn

Lei Wang

Institute of Computing Technology,  
Chinese Academy of Sciences  
University of Chinese Academy of  
Sciences  
wanglei\_2011@ict.ac.cn

Wanling Gao

Institute of Computing Technology,  
Chinese Academy of Sciences  
University of Chinese Academy of  
Sciences  
gaowanling@ict.ac.cn

Zihan Jiang

Institute of Computing Technology,  
Chinese Academy of Sciences  
University of Chinese Academy of  
Sciences  
jiangzihan@ict.ac.cn

Anzheng Li

Institute of Computing Technology,  
Chinese Academy of Sciences  
University of Chinese Academy of  
Sciences  
lianzheng20g@ict.ac.cn

Jianfeng Zhan\*

Institute of Computing Technology,  
Chinese Academy of Sciences  
University of Chinese Academy of  
Sciences  
zhanjianfeng@ict.ac.cn

## ABSTRACT

Classical machine learning (CML) occupies nearly half of machine learning pipelines in production applications. Unfortunately, it fails to utilize the state-of-the-practice devices fully and performs poorly. Without a unified framework, the hybrid deployments of deep learning (DL) and CML also suffer from severe performance and portability issues. This paper presents the design of a unified compiler, called CMLCompiler, for CML inference. We propose two unified abstractions: operator representations and extended computational graphs. The CMLCompiler framework performs the conversion and graph optimization based on two unified abstractions, then outputs an optimized computational graph to DL compilers or frameworks. We implement CMLCompiler on TVM. The evaluation shows CMLCompiler's portability and superior performance. It achieves up to 4.38 $\times$  speedup on CPU, 3.31 $\times$  speedup on GPU, and 5.09 $\times$  speedup on IoT devices, compared to the state-of-the-art solutions – scikit-learn, intel sklearn, and hummingbird. Our performance of CML and DL mixed pipelines achieves up to 3.04 $\times$  speedup compared with cross-framework implementations.

## CCS CONCEPTS

• Computing methodologies → Machine learning; • Computer systems organization → Real-time systems.

## KEYWORDS

Classical Machine Learning, Deep Learning, Compiler

## 1 INTRODUCTION

Deep learning (DL) and classical machine learning (CML), collectively called machine learning (ML), have played an increasingly critical role in recent years. DL refers to those neural network models, such as convolutional neural networks (CNNs) [24], recurrent neural networks (RNNs) [28], and generative adversarial networks (GANs) [16]. Different from DL, CML represents a set of non-neural network models in ML, e.g., linear models [37], decision trees [26],

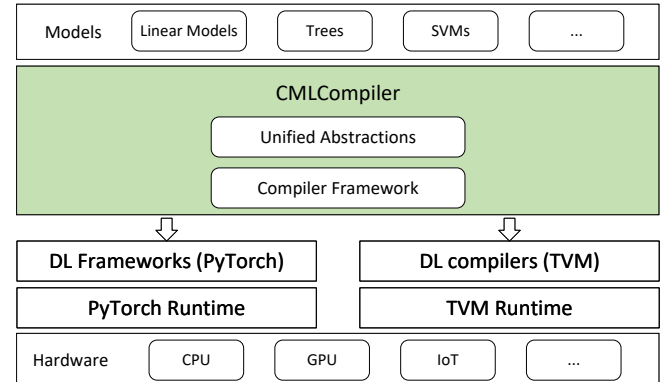


Figure 1: The CMLCompiler design. Our contributions are highlighted in green color.

random forests [4], and support vector machines [42]. DL stands out because of its accuracy, while CML is still widely used for lower time and energy costs. Doris Xin et al. [47] analyze 3000 production ML pipelines at Google and find that 40% of them use CML models. Besides, many real-world applications adopt hybrid deployments of CML and DL [2] to guarantee high accuracy and low latency [25, 27, 36, 38], e.g., DL models for feature embedding and CML models for classification or regression.

DL compilers, like TVM [7, 10, 23], provide a structural approach to tackle the portability issue and facilitates wide deployment of DL models on a broad spectrum of devices like GPUs, FPGAs, and IoT devices and guarantees an appreciable performance. DL compilers use computational graphs as high-level abstractions, supporting a large variety of DL models. Meanwhile, DL compilers propose low-level abstractions such as tensor representation to generate executable code. For newborn hardware, the vendor just need to provide hardware primitives, instead of a sophisticated high performance library that is prohibitively costly. Based on the tensor

\*Corresponding author.

representation and computational graphs abstractions, many optimizations [8, 22, 49] are proposed to boost performance, e.g., they provide sophisticated support for CPU processor architectures as the latter has different architectures, diverse core numbers, extended instructions, and cache sizes.

However, despite its popularity and importance, CML suffers from severe portability and performance issues. State-of-the-practice and state-of-the-art CML frameworks [17, 29, 32] provide ad-hoc solutions, implementing each CML model on every hardware device case by case due to the lack of unified abstractions. These ad-hoc solutions raise considerable difficulties in developing a general-purpose framework and optimization techniques to achieve optimal performance for every model. They either lack the support or only partially support various hardware devices, such as GPUs, FPGAs, and IoT devices. In addition, adding support for a model on a new hardware device needs great effort, more than several thousands of lines of codes [13], let alone hundreds or thousands of models and devices. Moreover, they also face performance issues. Even on the CPUs – the most popular CML platform, the performance is unsatisfactory due to the lack of specific optimizations for advanced characteristics like multi-cores and SIMD. The hybrid deployment of CML and DL models faces more severe problems.

Our intuition is to enable CML to leverage DL’s well-defined unified abstractions and highly mature compilers, optimization technologies, and frameworks. Unfortunately, it is not a trivial task. There are significant distinctions in operators and models between CML and DL. DL operators focus on tensors, while CML handles arrays, matrices, scalars, and tables. DL models are all neural network models, while CML models, such as decision trees and SVMs, can hardly be represented as neural networks. Most DL models are expressible as flat sequences of operations without if-statements [35], but if-statements frequently occur in CML models. Existing DL abstractions, such as tensor representation and computational graphs, can not directly represent CML operators and models. Those distinctions determine CML can hardly leverage the DL ecosystems directly. Several efforts attempt to support CML models on DL frameworks, e.g., TensorFlow [1] provides a CPU-based decision forest library TF-DF [43]. However, these attempts do not solve the generality and portability issue. They only support a narrower range of models, lacking support for GPUs and IoT devices.

This paper focuses on CML inference for the first step, considering its great significance that occupies nearly half of the total cost [2] and its wide applications in online serving, Internet of things (IoT), etc [18, 46]. We will extend our work to CML training in the near future. As illustrated in Fig. 1, we propose a unified compiler, CMLCompiler, for CML inference, which enables CML to leverage the mature DL ecosystems. At the core of CMLCompiler are two unified abstractions: operator representations and extended computational graphs (ECGs) and a compiler framework. Operator representations convert CML operators into tensor formats, while an ECG organizes these converted operators in an optimization-friendly way. The two unified abstractions define how to convert and translate CML models into DL computational graphs, which can be recognized and executed by DL frameworks and compilers. The CMLCompiler framework consists of four modules – operator converter, model parser, graph optimizer, and graph translator. The CMLCompiler framework performs the conversion and graph

optimization based on two unified abstractions, then outputs an optimized DL computational graph to DL compilers or frameworks. CMLCompiler can also optimize the mixed pipelines of CML and DL. As TVM provides portability and sophisticated optimizations, we choose to implement CMLCompiler on TVM. Currently, it supports up to 35 CML models.

This paper makes the following contributions:

- We propose two unified abstractions – operator representations and extended computational graphs– to represent CML operators and models.
- We present the design of CMLCompiler, a unified compiler for CML inference, based on these abstractions. The CMLCompiler framework performs the conversion and graph optimization based on two unified abstractions, then outputs an optimized DL computational graph to DL compilers or frameworks.
- CMLCompiler enables the hybrid deployment of CML and DL with a unified framework.
- We implement CMLCompiler on top of TVM, achieving up to 4.38x speedup on CPU, 3.31x speedup on GPU, and 5.09x speedup on IoT devices, compared to the state-of-the-art solutions – scikit-learn, intel sklearn, and hummingbird. Our support for CML and DL mixed pipelines achieves up to 3.04x speedup compared with cross-framework implementations.

The remainder of the paper is organized as follows. Section 2 introduces the motivation. Section 3 introduces unified abstractions. Section 4 shows design and implementation. Section 5 presents our evaluation. Section 6 illustrates the related work. Finally, we draw a conclusion in Section 7.

## 2 MOTIVATION

CML faces severe portability and performance issues. Fig. 2 compares the performance of sklearn, the most widely used CML framework on GitHub [33]—against CMLCompiler leveraging DL compilers. We find that sklearn can not support GPUs and only supports IoT devices partially. Adding support for a new hardware device needs great effort due to the ad-hoc implementations. For example, adding support for random forest on GPU needs 2.7k lines of code [13]. Many models and hardware devices need to be supported, requiring hundreds or thousands of more effort. Moreover, due to the lack of compilation support for CPU’s features, sklearn has poor performance. As shown in Fig. 2, CMLCompiler achieves 2.3x speedup by utilizing AVX2 through compilation compared with sklearn. Other CML frameworks such as Spark MLlib [29] and H2O [17] face the same problems. Our solution is to propose unified abstractions to utilize DL compilers and frameworks, achieving portability and high performance.

CML and DL models are often deployed hybrid in NLP [36], intelligent healthcare [38], recommendation systems [25], etc., especially in the scenarios with limited computational power and small datasets. Many of them are deployed on heterogeneous hardware devices for online serving. As there is no unified system, different frameworks are deployed with three disadvantages. First, this limits the portability. If one framework fails on the target device, the whole pipeline corrupts. Second, there are extra costs due to data

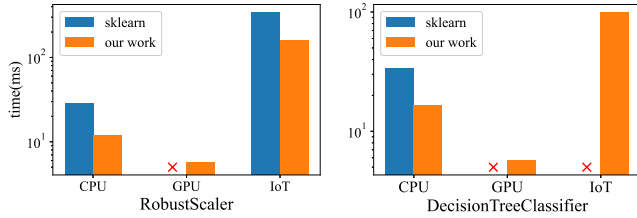


**Figure 2: This figure compares the performance of sklearn, the most widely used CML framework on GitHub [33]—against CMLCompiler. Our evaluation shows that sklearn suffers from both performance and portability issues for a lack of unified abstractions.**

conversions across frameworks. Third, it is hard to make optimizations across different frameworks. Using a unified framework can overcome these disadvantages, so we add the support for hybrid deployment of CML and DL in CMLCompiler.

### 3 THE UNIFIED ABSTRACTIONS

CMLCompiler takes CML models as input and returns DL computational graphs as output, utilizing DL frameworks or compilers to compile and deploy them. At the core of CMLCompiler are two unified abstractions. Operator representations are used to represent CML operators in tensor format, as shown in Section 3.1. Extend computational graph (ECG) organizes operator representations in an optimization-friendly way and can be used to represent CML models, as shown in Section 3.2. Section 3.3 shows the supported algorithms and extensions for other algorithms.

#### 3.1 Operator Representation

An operator representation uses a combination of one or more DL operators with tensors as input and output to represent a CML operator. We convert CML operators into DL operators and wrap them in the format of operator representations. Data in CML has mainly four formats: arrays, matrices, scalars, and tables [44]. Matrices and arrays are regarded as two types of tensors whose operators can naturally be converted into DL operators. When CML models deal with tables, they take numeric data from tables and operate it, which can also be regarded as scalars. Hereby, we focus on the operators on scalars.

**3.1.1 Operator categories and corresponding representations.** As shown in Table 1, we classify CML operators into six categories and provide operator representations, respectively.

(1) Assignment operators assign values to variables. If we assign  $n$  values  $v_1, v_2, \dots, v_n$  to  $n$  variables  $x_1, x_2, \dots, x_n$ , we organize these variables and values in two tensors  $X = [x_1, x_2, \dots, x_n]$  and  $V = [v_1, v_2, \dots, v_n]$ . Then we assign tensor  $V$  to tensor  $X$  to replace  $n$  scalar assignments. Tensor assignments benefit memory copy which stores data in block.

(2) Swap operators swap two or more variables. These variables can be represented in a tensor format and use reorganization operators such as *reshape* to swap the elements.

(3) Basic arithmetic operators refers to those arithmetic calculations based on scalars, such as *add*, *sub*, *mul* and *div*. We use

element-wise arithmetic operators based on tensors to replace them, which can utilize SIMD instructions better.

(4) Aggregation operators refer to operators that calculate aggregates among many scalars, such as *min*, *max*, *sum*, and *avg*. Reduction operators can be used to accomplish that.

(5) Comparison operators make a comparison between scalars and return True or False, such as *less*, *equal*, and *greater*. Comparisons with the same operator can be represented in a tensor format and use an element-wise comparison to replace.

(6) Conditional operators are used to represent if-else statements, in the form of *if*(*expr1*) *expr2* *else* *expr3*, where *expr1* is a comparison operator. If *expr2* and *expr3* are all assignment or arithmetic operators, we convert all three expressions into tensors. However, the situation gets tricky if one of *expr2* or *expr3* is still a conditional operator. We call those operators sequential conditional operators. Sequential conditional operators may contain many conditions, where each element in a tensor may have quite different decision paths. The complexity of decision paths makes it difficult to convert those operators into tensor operators. Those frequent if-else statements perform poorly on hardware devices such as GPUs and ASICs. Sequential conditional operators are the most delicate, and we defer their discussion later.

**3.1.2 Conditional operators representation.** We analyze those widely used CML models and find that sequential conditional operators mainly occur in tree-based models. So we use decision tree as an example to introduce the representation of conditional operators in detail, as shown in Fig. 3. We use the combination of DL operators to represent those sequential conditional operators.

The left is a decision tree. The input data is a list of samples; each has many features.  $I$  refers to internal nodes, numbered in the order of Level Order Traversal. Each internal node is a conditional operator, making a comparison between a feature  $F_j$  and a constant threshold  $T_i$ .  $L$  refers to leaf nodes, numbered in the order of In-Order Traversal. Each leaf node is an assignment operator, reaching which node determines the final result.

The right in Fig. 3 shows the operator representation, whose definitions and properties of weights are shown in Table 2. Input data multiplied by  $W_1$  returns those features used in internal nodes in an appropriate order. Comparing with  $W_2$  returns the choice of each internal node: 0 means left and 1 means right. These choices are multiplied by  $W_3$  and then use *argmax* to return the first index of the maximum values for each row. For each sample  $x_k$ , that index is the leaf node  $x_k$  reaches, as proved in appendix A.

**3.1.3 The features of CML operator representations.** As described above, we represent CML operators in the format of operator representations. These operator representations have unique features different from operators in DL models.

First, the weights of DL operators and CML operator representations have different meanings. The weights in DL models are all learnable parameters. Without approximate optimizations such as pruning and quantization, those weights are dense, and the data type (dtype) should be float32 to ensure accuracy. Many weights of CML operator representations have other meanings, such as representing the structure of conditional operators. Those weights are sparse and can naturally be expressed as low-precision dtypes such

**Table 1: The summary of operator representation. Each operator representation represents a CML operator. Scalars are marked as lower-case letters, while tensors are marked as upper-case letters. EW is short for element-wise.**

CML operators in scalar format		Operator Representation in tensor format	
Operator Type	Expressions	Operator Type	Expressions
Assignment	$x_1 \leftarrow v_1; x_2 \leftarrow v_2; \dots; x_n \leftarrow v_n$	Assignment	$X = [x_1, x_2, \dots, x_n]; V = [v_1, v_2, \dots, v_n]; X \leftarrow V$
Swap	$x_1 \leftarrow x_2; x_2 \leftarrow x_1;$	Reorganization	$X = [x_1, x_2]; \text{reshape}(X);$
Basic Arithmetic	$x_1 + y_1; x_2 + y_2; \dots; x_n + y_n$	EW Arithmetic	$X = [x_1, x_2, \dots, x_n]; Y = [y_1, y_2, \dots, y_n]; X + Y$
Aggregation	$\text{sum}(x_1, x_2, \dots, x_n)$	Reduction	$X = [x_1, x_2, \dots, x_n]; \text{sum}(X)$
Comparison	$x_1 < y_1; x_2 < y_2; \dots; x_n < y_n$	EW Comparsion	$X = [x_1, x_2, \dots, x_n]; Y = [y_1, y_2, \dots, y_n]; X < Y$
Conditional	$\text{if}(expr1) expr2 \text{ else } expr3$	Described in Section 3.1.2	

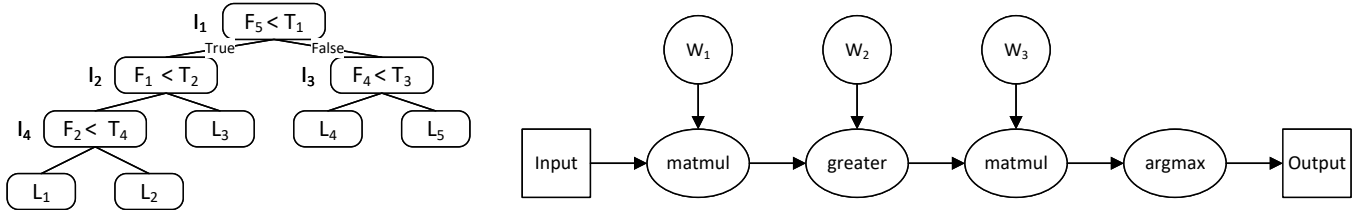


**Figure 3: An example of conditional operator representation in decision tree, a typical classical machine learning model.  $F$ ,  $T$ ,  $I$ , and  $L$  refer to features, thresholds, internal nodes, and leaf nodes.  $W_1$ ,  $W_2$ , and  $W_3$  are the weights of DL operators, whose definitions and properties are shown in Table 2, matmul is short for matrix multiplication.**

**Table 2: The properties of weights in Fig. 3.**  $N_S$ ,  $N_F$ ,  $N_I$ , and  $N_L$  refer to the number of samples, features, internal nodes, and leaf nodes, respectively.  $\text{Input} \in \mathbb{R}^{N_S \times N_F}$  means  $N_S$  samples, each has  $N_F$  features.  $W_1 \in \{0, 1\}^{N_F \times N_I}$  captures the relationship between features and internal nodes.  $W_2 \in \mathbb{R}^{N_I}$  is the thresholds used in internal nodes.  $W_3 \in \{0, 1\}^{N_I \times N_L}$  represents the structure between internal nodes and leaf nodes.  $\text{Output} \in \mathbb{N}^{N_S}$  returns the leaf node index each sample reaches.  $\text{Dtype}$  is the data type of weights.  $\text{Sparsity}$  is the ratio of non-zero data to all data in weights.

Definition	Dtype	Sparsity
$W_1[i][j] = \begin{cases} 1, & F_i \in \text{Condition}(I_j) \\ 0, & \text{otherwise} \end{cases}$	bool	$\frac{1}{N_F}$
$W_2[i] = \text{Threshold}(I_i)$	float32	1
$W_3[i][j] = \begin{cases} 0, & L_j \in \text{LeftSubTree}(I_i) \\ 1, & \text{otherwise} \end{cases}$	bool	$[\frac{1}{2}, 1 - \frac{1}{N_L}]$

as bool. The natural sparse features bring optimizations described in Section 4.3.2.

Second, the frequent operators in DL and CML are not the same. Almost all operators in DL take float32 as input and return float32 as output. CML uses many comparison operators, such as *less*, *equal*, and *greater*, which rarely occur in DL models. Those comparison operators take float or integer as input and return bool tensors, bringing remarkable changes in the dtype of input and output, which can be used to make optimizations as described in Section 4.3.1. Both DL and CML models use indices operators, which compare input and returns indices, such as *argsort* and *argmax*.

Those indices operators have mathematical properties that can be used to make graph-level optimizations, as described in Section 4.3.3. These optimizations can be ignored in DL models with dozens or hundreds of layers but are helpful for those CML models with fewer layers.

### 3.2 Extended Computational Graph

This section introduces extended computational graph (ECG), which organizes operator representations in an optimization-friendly way and can be used to represent CML models. ECG is an extension based on DL computational graph. In general, a DL computational graph is represented as a directed graph where nodes represent operations on tensors or program inputs and edges represent data dependencies between operations [7]. From a perspective of the DL frameworks and compilers, computational graphs are dense and float32 by default, such as neural network models. Using approximate optimizations like pruning and quantization brings sparse and low-precision data to all operators and weights. These optimizations cause a decrease in accuracy and bring extra computation, such as calibration. When we convert CML operators to operator representations, part of those converted operators and weights are sparse and low-precision naturally. Using DL computational graphs to represent CML models directly is not precise enough and ignores many optimization opportunities due to the data type and sparse features. So we extend the computational graph in the DL systems into extended computational graph (ECG) as the unified abstraction for CML models.

Before introducing ECG, first, we present more details about data type (dtype) and sparsity. We define the partial order relation for dtypes used in our work:

$$\text{float32} > \text{int32} / \text{float16} > \text{int16} > \text{int8} > \text{int4} > \text{bool}$$

**Table 3: Operators used in ECGs**

Operator Type	Examples
Comparison	less, equal, greater, less_equal
Indices	argmax, argmin, argsort, argwhere
Monotonic	sigmoid, softmax, relu, tanh, exp
Reduction	sum, max, min, avg, all, any
Arithmetic	gemm, conv, pool

The lower dtype can be converted into a higher dtype without accuracy loss, while a backward conversion with accuracy loss is forbidden. Using lower dtype computation, such as int8 matmul, can speed up and reduce memory usage. However, there are many limitations to dtype optimization. For example, the inputs of the same operator should have the same dtype; thus, the dtype of operators depends on the largest dtype of inputs. Besides, many hardware devices have extended instructions based on specific dtypes. For example, an Intel processor speeds up int8 computation using AVX instruction, while bool cannot benefit from that. Considering the complexity of dtype optimization, we add dtype as a property for ECG.

Sparsity is defined as the ratio of non-zero data to all data. If data sparsity is relatively small, we take it as sparse data and store it in a compressed sparse row (CSR) format. Using sparse operators to handle those sparse data can perform better than dense operators. Taking advantage of sparsity influences optimization greatly, so we add sparsity as another property for ECG.

We classify the inputs of an operator into two categories: intermediate results and weights. Intermediate results are other operators' outputs and can only be handled during runtime. Input data is the first intermediate result in ECG, while output data is the last. Intermediate results are represented as  $\{sparsity, dtype, tensor\}$ . If we want to change the dtype of intermediate results, we should add dtype converting operator in the ECG.

Weights are model parameters that can be loaded from trained models. Weights can be handled both during compilation and runtime, while a proper transformation during compilation can reduce runtime costs. Weights are represented as  $\{sparsity, smallest\_dtype, actual\_dtype, tensor\}$ . Smallest\_dtype is the smallest dtype for weights without accuracy loss, actual\_dtype is the dtype actually used. Smallest\_dtype depends on the property of weights, while actual\_dtype is fixed based on smallest\_dtype and operators. As shown in Fig. 3,  $W_1$  represents the relationship between input features and internal nodes for decision trees, which is a 0-1 matrix. The smallest\_dtype of  $W_1$  is bool. However,  $W_1$  is multiplied by input data with a dtype of float32. If we choose bool as the actual\_dtype,  $W_1$  will be converted to float32 during runtime. To reduce the execution time in runtime, we should convert  $W_1$  to float32 during compilation, so we set actual\_dtype as float32 rather than bool.

Operators are represented in the form of  $\{weights, intermediate\_results, use\_sparse, type, dtype, DL\_operator\}$ . Weights and intermediate\_results are inputs of operators. Use\_sparse is a flag of whether using the sparse operator or not, which is closely related to sparse operator replacing optimization described in Section 4.3.2. Operator type is the type of operator. As shown in Table 3, we

**Table 4: Supported Algorithms**

Preprocessing Algorithms
Binarizer, LabelBinarizer, Normalizer, MaxAbsScaler, MinMaxScaler, StandardScaler, RobustScaler, PolynomialFeatures, LabelEncoder
Feature Selectors
SelectKBest, VarianceThreshold
Linear Models
LogisticRegression, LogisticRegressionCV, Perception, RidgeClassifier, RidgeClassifierCV, SGDClassifier, LinearRegression, Ridge, RidgeCV, SGDRegressor
Tree-based Models
DecisionTreeClassifier, DecisionTreeRegressor, ExtraTreeClassifier, ExtraTreeRegressor, RandomForestClassifier, RandomForestRegressor, ExtraTreesClassifier, ExtraTreesRegressor, GradientBoostingClassifier, GradientBoostingRegressor
Support Vector Machines
LinearSVC, LinearSVR, NuSVR, SVR

divide operators used in ECG into five categories. Comparison operators refer to those operators that compare two tensors and return bool tensors. Indices operators refer to those operators that return tensors' indices based on specific conditions. Those two kinds of operators are dtype-lowering operators, the output dtype of which is smaller than the input. Models without those operators, such as most DL models, use the same dtype through the whole graphs, where dtype optimizations cannot be used without approximate optimization. CML models make much use of those operators, which have wide usage of dtype rewriting optimization described in Section 4.3.1. Monotonic operators refer to those operators who meet the following conditions:

$$\forall x_1 \leq x_2 \implies f(x_1) \leq f(x_2)$$

A series of monotonic operators followed by an indices operator is mathematically equivalent to the indices operators alone. Those properties provide more optimizations, as described in Section 4.3.3. Reduction operators calculate aggregates over input. Arithmetic operators refer to other arithmetic calculations. Operator dtype is the operators' data type, such as int8 matmul or float32 matmul. Operator dtype depends on the dtype of weights and intermediate\_results. DL\_operator is the native definition of operators in DL computational graphs, which we use to translate ECG to DL computational graphs.

### 3.3 Supported Algorithms and Extension for Other Algorithms

CMLCompiler supports 35 CML algorithms nowadays, as shown in Table 4, covering most of the popular CML algorithms [34]. Our work can also be extended to other algorithms, such as clustering and matrix decomposition. Most CML algorithms use operators categorized in Section 3.1.1, each of which can be converted to corresponding Operator Representations—our low-level abstractions, guaranteeing our extensibility. We take Kmeans as an example.

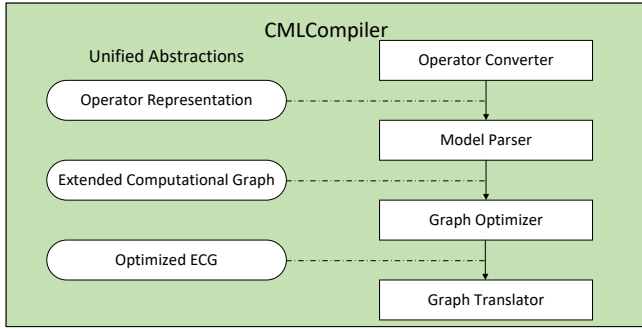


Figure 4: The CMLCompiler architecture.

Kmeans use basic arithmetic operators to calculate the distance between nodes, which can be converted to element-wise arithmetic operators and use aggregation operators to make clustering, which can be converted to reduction operators. When all operators of a CML algorithm are converted to Operator Representations, it can utilize our work to compile and make optimizations.

## 4 DESIGN AND IMPLEMENTATION

This section illustrates the design and implementation of CMLCompiler, as shown in Fig. 4. We build our framework based on the two unified abstractions, including four parts. Operator Converter converts CML operators into operator representations, as shown in Section 4.1. Model Parser organizes those operator representations in an optimization-friendly way and uses ECGs to represent CML models, as shown in Section 4.2. Graph Optimizer makes graph level optimizations, as described in Section 4.3. An optimized ECG is converted into a DL computational graph by Graph Translator in Section 4.4. DL frameworks or compilers take DL computational graphs as input and make more optimizations, compiling them into executable modules to deploy. Section 4.5 shows the mixture usage of CML and DL. Section 4.6 shows the implementation details.

### 4.1 Operator Converter

Operator Converter traverses the operators in CML models and converts them into operator representations, respectively. Operators based on matrices and arrays are converted into DL operators directly. Scalar-based operators are converted into DL operators based on their categories, according to Section 3.1. These converted DL operators are wrapped into operator representations.

### 4.2 Model Parser

Model Parser converts operator representations into an ECG, as shown in Algorithm 1. Operators in an operator representation are initialized as nodes in an ECG, the data structure of which is defined in Section 3.2. Operator.weights and operator.intermediate\_results are set according to data dependencies, and edges are built between nodes. Operator.use\_sparse and operator.dtype are set as False and Unknown, respectively. Operator.type is set according to operator type, which is defined in Table 3. Then weights and intermediate\_result are initialized. Weight.sparsity is set as the ratio of non-zero data and all data for weight, known during compilation.

Weight.smallest\_dtype is set as the smallest dtype without accuracy loss, and weight.actual\_dtype is initialized the same. Intermediate\_result.sparsity and intermediate\_result.dtype are set according to operator. When all operators are visited, the ECG is established.

---

#### Algorithm 1 Model Parser

---

```

Input: Operator Representation
Output: Extended Computational Graph ECG
for operator in Operator Representation do
    Initialize operator as ECG node
    Set operator.weights and operator.intermediate_results according to data dependencies and build edges between nodes
    operator.use_sparse  $\leftarrow$  False
    operator.type  $\leftarrow$  operator type
    operator.dtype  $\leftarrow$  Unknown
    for weight in operator.weights do
        weight.sparsity  $\leftarrow$  the ratio of non-zero data and all data
        weight.smallest_dtype  $\leftarrow$  the smallest dtype without accuracy loss
        weight.actual_dtype  $\leftarrow$  weight.smallest_dtype
    end for
    for ir in operator.intermediate_results do
        set ir.sparsity and ir.dtype according to operator
    end for
end for

```

---

### 4.3 Graph Optimizer

Graph Optimizer performs graph-level optimizations, using a functionally equivalent transformation for ECGs. These optimizations are based on the features of CML models and do not influence accuracy. There are three specific graph rewriting optimizations: dtype rewriting, sparse operator replacing, and redundant elimination.

**4.3.1 Dtype rewriting.** Dtype rewriting uses low precision computation with faster speed and less memory to replace high precision computation. As analyzed in Section 3.1.3, many weights used in CML can be represented as bool or int8. Besides, comparison operators and indices operators widely used in CML are dtype-lowering operators. The intermediate results after those operators are bool or int8. When intermediate data and weights can be both expressed as low precision dtype, the corresponding operators can be converted into low precision computation as well.

As shown in Fig. 5a, the top is the ECG of decision trees before optimization; many details are hidden. Weight  $W_3$  represents the relationship between leaf nodes and internal nodes for decision trees, which is a matrix only containing 0 and 1. The smallest\_dtype of  $W_3$  is bool. The output of *greater* operator has a dtype of bool as well. So the following matrix multiplication (matmul) operator can use a dtype of bool rather than float32. Intel processors speed up int8 computation using AVX instruction, while bool cannot benefit from that feature. So we convert the dtype of matmul to int8 according to hardware specification. In Fig. 5a, the below is the ECG after graph rewriting. Those white weights and operators use float32, while gray weights and operators use int8.

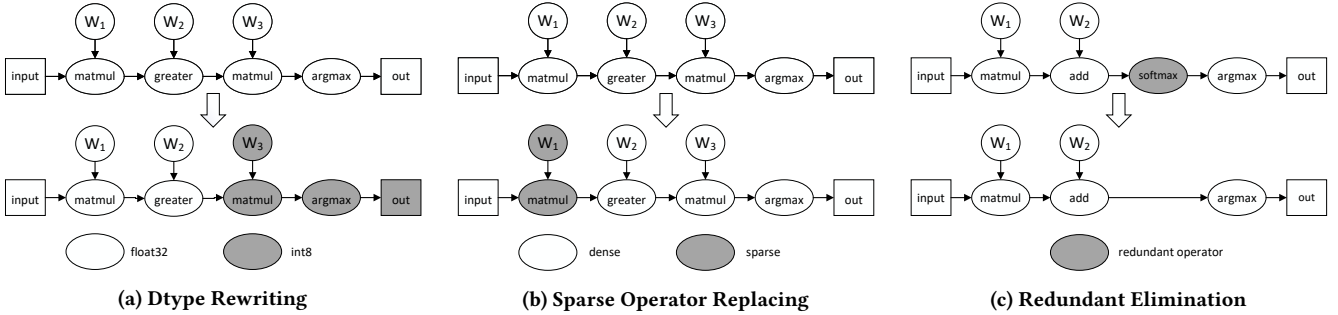


Figure 5: Graph rewriting optimizations. Dtype rewriting converts float32 operators and weights into low-precision. Sparse operator replacing converts dense operators and weights into sparse. Redundant elimination reduces redundant operators.

Now we introduce the dtype rewriting principle in detail. Algorithm 2 shows the procedure of dtype rewriting:

(1) Visit all operators in ECG. For each operator, dtype is set as the largest dtype of all inputs. After that, operator dtype is converted to the dtype which can utilize hardware’s SIMD instructions best. We keep a list of hardware specifications to modulate operator dtype. In order to guarantee accuracy, dtype cannot get smaller. Then we modulate operator implementation based on operator dtype.

(2) When operator dtype is fixed, we set the input dtype. The dtype of weights is set the same as the operator, reducing dtype conversion in runtime. The dtype of intermediate results cannot be converted during compilation. So we add dtype converting operator, i.e, cast, before the operator.

We explain the differences between dtype rewriting for CML models and model quantization for DL models. Quantization is an approximate algorithm for DL models that causes a decrease in accuracy and brings extra computation, such as calibration. Dtype rewriting for CML models is based on the properties of CML, converting dtype of operators and weights with no accuracy decrease and extra computation.

---

#### Algorithm 2 Dtype Rewriting

---

**Input:** ECG  $G$ , hardware configuration  $H$

**Output:** Optimized ECG  $G'$

```

for operator in  $G$  do
    operator.dtype  $\leftarrow$  largest dtype in operator.weights and operator.intermediate_results
    Modulate operator.dtype based on  $H$ 
    Modulate operator.DL_operator based on operator.dtype
    for weight in operator.weights do
        weight.actual_dtype  $\leftarrow$  operator.dtype
    end for
    for data in operator.intermediate_results do
        if data.dtype < operator.dtype then
            Add cast(data, operator.dtype) before operator
        end if
    end for
end for

```

---

4.3.2 *Sparse operator replacing*. Replacing dense operators with sparse operations can speed up as well. Algorithm 3 shows the

procedure of sparse operator replacing. The sparsity of input data can be known until runtime, while the sparsity of weights can be known during compilation. So we convert the data format of weights rather than input data. Different hardware devices have different support for sparse operators. For example, CPUs can benefit from sparse computation while GPUs have little effect. So we set a threshold based on hardware specification. If weight sparsity is smaller than the threshold, we store it in a compressed sparse row (CSR) format. Then we convert the corresponding operator into a sparse implementation. An example is shown in Fig. 5b, we convert  $W_1$  and the corresponding matmul to sparse.

---

#### Algorithm 3 Sparse Operator Replacing

---

**Input:** ECG  $G$ , Threshold  $T$

**Output:** Optimized ECG  $G'$

```

for operator in  $G$  do
    for weight in operator.weights do
        if weight.sparsity <  $T$  then
            Store weight into CSR format
            operator.use_sparse  $\leftarrow$  True
            Convert operator.DL_operator into sparse implementation
        end if
    end for
end for

```

---

4.3.3 *Redundant elimination*. Redundant elimination eliminates those operators who do not influence final results due to their mathematical properties. For example, a series of monotonic operators followed by an indices operator is mathematically equivalent to the indices operators alone. Algorithm 4 shows the procedure of redundant elimination. For each operator in ECGs, we check its operator type. If another monotonic operator follows a monotonic operator, we fuse them. We eliminate the monotonic operator if it is followed by an indices operator. An example is shown in Fig. 5c, the softmax before argmax is eliminated.

#### 4.4 Graph Translator

Graph Translator converts the optimized ECG into DL computational graph, choosing the proper implementation based on ECG

**Algorithm 4** Redundant Elimination

---

**Input:** Extended Computational Graph  $G$   
**Output:** Optimized ECG  $G'$

```

for operator in  $G$  do
  if operator.type == "monotonic" then
    Check the next operator operator'
    if operator'.type == "monotonic" then
      Merge operator and operator'
    else if operator'.type == "indices" then
      Eliminate operator
    end if
  end if
end for

```

---

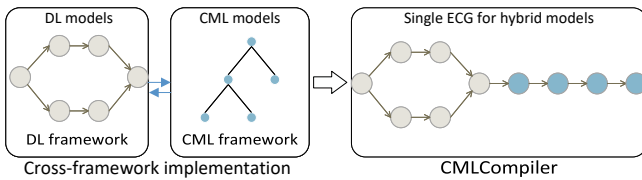


**Figure 6:** CMLCompiler uses a single ECG to represent CML and DL mixed pipeline.

and hardware specification information. DL frameworks or compilers, like TVM, take DL computational graphs as input and make more optimizations, finally compiling them into executable modules.

#### 4.5 Hybrid Deployment of CML and DL with a Unified Framework

We convert those CML and DL hybrid applications under a unified framework to reduce the cost of switching frameworks and provide an opportunity for end-to-end optimizations, as shown in Fig. 6. We load models from PyTorch and sklearn and convert them into ECG subgraphs. We build edges according to data dependency and merge those subgraphs in a single ECG. Then we can use optimizations both in our work and DL compilers. Finally, we compile and deploy it on diverse hardware devices.

#### 4.6 Implementation

Due to the benefits in portability and performance, we implement CMLCompiler on the basis of TVM. The intermediate representations and transforms are all written in python. We read trained models from CML frameworks such as sklearn and convert them into operator representations, implementing them in the format of TVM relay functions and storing their weights in TVM arrays. We wrap those relay functions in the format of ECGs. After optimizations in Section 4.3, we convert ECGs into TVM's IRModules. Then we utilize TVM to make more optimizations and compile to executable modules based on specific hardware targets. We use cross-compilation to support a broad spectrum of hardware devices. We deploy them on lightweight runtime based on TVM runtime and make inference on various hardware devices.

## 5 EVALUATION

This section summarizes the evaluation. Section 5.1 shows experimental setup. Section 5.2 evaluates the performance of graph rewriting optimizations based on ECGs. Section 5.3 compares our work with the state-of-the-art frameworks. Section 5.4 evaluates the hybrid deployment of CML and DL.

### 5.1 Experimental Setup

We deploy a server node equipped with two Xeon E5-2620 V3 (Haswell) CPUs, an Nvidia Titan RTX GPU, and 64 GB memory to conduct the experiments on CPU and GPU. Each CPU contains six physical cores. The GPU contains 4608 Cuda cores and 24 GB memory. The operating system is Ubuntu 16.04, and the other software includes TVM 0.8, PyTorch 1.8.1, hummingbird 0.3.1, scikit-learn 1.0.1, and CUDA 10.2. For the IoT experiments, we use Raspberrypi4b with Raspbian 10 operating system and deploy the above software with the same version. We use YearPrediction [12] as the dataset, with 515345 samples and 90 features. We use 80% data to train models and 20% data to make inference. We run all the experiments five times and use the average as the final results. We test hummingbird [30] using both two backends (PyTorch and TVM) and select their best results.

### 5.2 Optimizations

This section evaluates graph rewriting optimizations based on ECGs, as described in Section 4.3. These optimizations: dtype rewriting, sparse operator replacing, and redundant elimination, can work together and produce cumulative optimization effects. They can also coexist with the optimizations in TVM. We choose four typical tree models: DecisionTreeClassifier, RandomForestClassifier, ExtraTreeClassifier, and ExtraTreesClassifier, as well as two typical linear models: LogisticRegression and SGDClassifier. We evaluate the dtype rewriting and sparse operator replacing for tree models, and redundant elimination for linear models according to their unique patterns.

Fig. 7a shows the result on CPU. For tree models, using our work without optimizations has a 1.31x-2.54x speedup compared with sklearn; this is due to our abstractions which utilize optimizations of TVM, including better utilization of SIMD instructions and multi cores. Using dtype rewriting and sparse operator replacing bring 1x-1.21x and 1.26x-1.75x speedup, respectively, achieving 1.27x-2.11x speedup together, 1.84x-4.44x faster than sklearn. For linear models, our work without optimizations runs slower than sklearn. However, using redundant elimination brings 1.22x-1.51x speedup; the result after our optimizations is 1.06x-1.14x faster than sklearn.

Fig. 7b shows the result of IoT devices. Note that sklearn lacks enough support for IoT devices. For example, 64-bit tree models trained on servers cannot be executed on Raspberrypi4b with a 32-bit operating system. Retraining those models in 32-bit format on Raspberrypi4b from scratch takes more time, so we regard those models as unsupported, marked as cross. So we take our work without optimizations as the baseline. Using dtype rewriting and sparse operator replacing bring 1.01x-1.33x and 1.23x-2.3x speedup, respectively, achieving 1.49x-2.53x speedup together. For linear models,

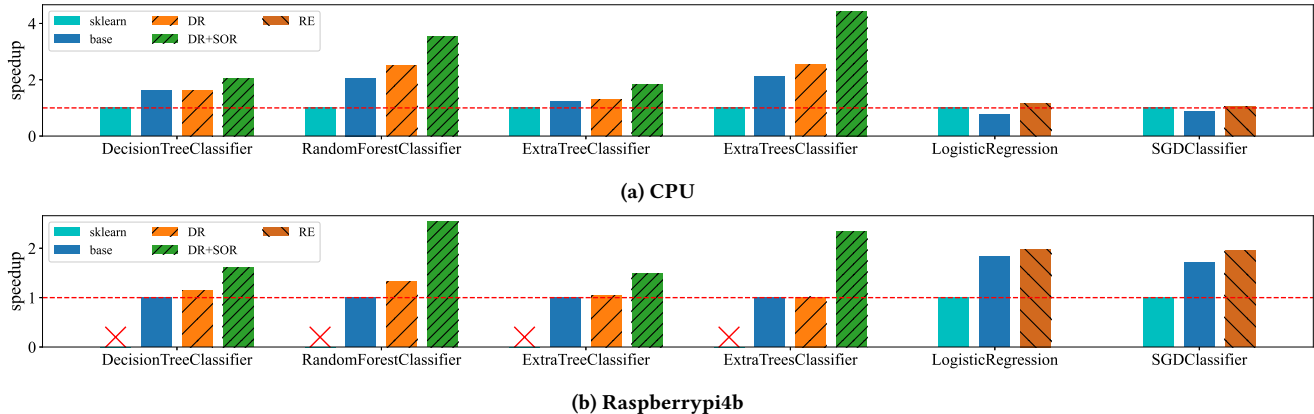


Figure 7: Graph Rewriting Optimizations. "base" means our work without optimizations. "DR" means only using dtype rewriting. "DR+SOR" means using both dtype rewriting and sparse operator replacing. "RE" means using redundant elimination.

our work without optimizations achieves 1.71x-1.84x speedup. Using redundant elimination brings 1.08x-1.14x more speedup, 1.95x-1.98x faster than sklearn. The computation part of GPU is less than 20%, so those optimizations play a limited role on GPU. In conclusion, CML models can benefit from both TVM’s optimizations and our optimizations and achieve obvious speedup.

### 5.3 Overall Results

This section evaluates 14 typical CML algorithms covering preprocessing algorithms, linear models, tree-based models, and SVMs, on CPU, GPU, and IoT devices, compared with state-of-the-art frameworks including sklearn, intel extension for sklearn [20], and hummingbird. It contains two parts: batch experiments for all data and query experiments for a single record.

The differences between the accuracy of CMLCompiler and sklearn are all less than  $1 \times 10^{-5}$ , which means that our work does not affect the accuracy. The outputs on different hardware are all the same, so we focus on performance hereinafter. Table 5 shows the performance of batch experiments. On CPU, our work reflects the best performance on 12 algorithms out of 14, achieving 1.02x-10.57x speedup compared with sklearn, 1.14x-4.38x speedup compared with hummingbird, and 1.44x-8.47x speedup compared with intel sklearn. On GPU, our work achieves competitive performance compared with hummingbird. Our work performs better on 11 algorithms out of 14, with a 1.11x-3.31x speedup. On an IoT device RaspberryPi4b, our work performs better on 13 algorithms out of 14, with a 1.28x-5.09x speedup.

Table 6 shows the performance of query experiments for a single record. On CPU, our work achieves the best performance on 11 algorithms out of 14, with a 1.36x-170.68x speedup compared with sklearn, a 1.56x-4.47x speedup compared with hummingbird, and a 1.31x-169.43x speedup compared with intel sklearn. Our work has better performance on GPU on 10 algorithms out of 14 compared with hummingbird, with a 1.41x-4.64x speedup. Our latency on RaspberryPi4b does not differ much compared with sklearn. However, we perform better in model support.

In conclusion, we have advantages in both batch and query experiments for all three hardware devices. Many models in sklearn

only support a single core and cannot fully utilize the SIMD instructions. We perform better than sklearn and intel sklearn due to better utilization of multi cores and SIMD instructions through compilation. Hummingbird uses both PyTorch and TVM as backends, where TVM performs better in most cases of our evaluations. It implements models in PyTorch and converts them into TVM using *from\_pytorch* API. This conversion is not direct and efficient enough, causing a performance decrease. Besides, hardware information is missed during conversion, which limits the optimizations of TVM for hummingbird. We map ECGs into relay operators directly and select the most efficient implementation based on ECGs and hardware specification information. Additionally, our abstractions bring more optimizations, as described in Section 4.3, bringing up to 2.53x speedup, working together to achieve better performance.

### 5.4 Hybrid Deployment of CML and DL

This section shows three hybrid deployment cases of CML and DL. As the baselines, without a unified framework, a DL framework is used to implement DL algorithms, while a CML framework is used to implement CML algorithms. Our work converts CML and DL models into a single ECG, making optimizations and compiling to diverse hardware devices. We test the latency of a single query, which is essential in real-world applications.

**5.4.1 Sentence Sentiment Classification.** The first one is a sentence sentiment classification case, which uses Bert to embed English sentences and logistic regression to make a classification [36]. We use BERT-tiny [3] as the pre-trained Bert model and SST2 [40] as the dataset. The baseline implements BERT-tiny in pytorch-transformers [45] and logistic regression in sklearn. The result is shown in Fig. 8a. Our work achieves a 1.67x speedup on server CPUs. Pytorch-transformers cannot be installed on IoT devices, so the baseline cannot run on RaspberryPi4b. The latency of our work on RaspberryPi4b is 18 milliseconds, which is acceptable in most use cases.

**5.4.2 Radiographic Image Analysis.** The second case uses Deep Hybrid Learning [38] to analyze radiographic images, which uses

**Table 5: Execution time for batch experiments over all data on CPU (12 cores), GPU, and IoT devices (take RaspberryPi4b as an example) in milliseconds. SK, HB, and Intel is short for scikit-learn, hummingbird, and Intel extension for sklearn, respectively. “-” means unsupported.**

Algorithm	CPU				GPU		IOT	
	SK	HB	Intel	Our	HB	Our	SK	Our
Binarizer	97	31	77	<b>9</b>	19	<b>6</b>	634	<b>126</b>
Normalizer	25	33	<b>15</b>	<b>15</b>	7	<b>5</b>	241	<b>168</b>
MinMaxScaler	19	31	13	<b>8</b>	21	<b>6</b>	199	<b>148</b>
RobustScaler	28	32	25	<b>12</b>	19	<b>5</b>	343	<b>156</b>
LinearRegression	12	18	<b>4</b>	6	<b>6</b>	7	<b>61</b>	116
LogisticRegression	98	104	137	<b>86</b>	7	7	1889	<b>952</b>
SGDClassifier	94	98	139	<b>88</b>	9	7	1886	<b>969</b>
DecisionTreeClassifier	33	48	23	<b>16</b>	7	<b>5</b>	-	<b>99</b>
DecisionTreeRegressor	7	19	<b>3</b>	15	7	<b>6</b>	-	<b>211</b>
RandomForestClassifier	2130	885	2003	<b>601</b>	<b>20</b>	-	-	<b>5820</b>
ExtraTreeClassifier	29	-	26	<b>16</b>	-	<b>6</b>	-	<b>206</b>
ExtraTreesClassifier	10022	2522	9421	<b>2256</b>	<b>99</b>	-	-	<b>47959</b>
LinearSVC	92	122	152	<b>77</b>	9	<b>6</b>	1896	<b>930</b>
LinearSVR	39	26	34	<b>5</b>	6	<b>5</b>	323	<b>112</b>

**Table 6: Latency for query experiments over one single record on CPU (12 cores), GPU, and IoT devices (take RaspberryPi4b as an example) in milliseconds. The symbols are the same as Table 5.**

Algorithm	CPU				GPU		IOT	
	SK	HB	Intel	Our	HB	Our	SK	Our
Binarizer	0.2	0.26	0.34	<b>0.09</b>	0.93	<b>0.64</b>	<b>0.44</b>	0.59
Normalizer	0.32	0.26	0.28	<b>0.11</b>	<b>0.25</b>	0.68	0.59	<b>0.41</b>
MinMaxScaler	0.15	0.31	0.14	<b>0.09</b>	0.91	<b>0.63</b>	<b>0.33</b>	0.37
RobustScaler	0.14	0.22	0.14	<b>0.11</b>	1.02	<b>0.72</b>	<b>0.37</b>	<b>0.37</b>
LinearRegression	0.24	0.35	0.32	<b>0.1</b>	0.91	<b>0.55</b>	<b>0.52</b>	0.69
LogisticRegression	0.35	0.36	0.29	<b>0.19</b>	3.29	<b>0.71</b>	<b>0.67</b>	2.59
SGDClassifier	0.4	0.35	0.29	<b>0.23</b>	2.93	<b>0.67</b>	0.68	<b>0.65</b>
DecisionTreeClassifier	<b>0.24</b>	1.62	0.27	0.36	3.01	<b>0.8</b>	-	<b>0.9</b>
DecisionTreeRegressor	<b>0.22</b>	<b>0.22</b>	0.25	0.38	1.03	<b>0.72</b>	-	<b>0.88</b>
RandomForestClassifier	103.96	1.6	103.2	<b>0.61</b>	<b>2.56</b>	-	-	<b>1.05</b>
ExtraTreeClassifier	<b>0.23</b>	-	0.4	0.47	-	-	-	<b>1.81</b>
ExtraTreesClassifier	205.27	12.74	204.25	<b>1.73</b>	<b>2.41</b>	-	-	<b>3.11</b>
LinearSVC	0.4	0.37	0.45	<b>0.19</b>	2.71	<b>0.61</b>	<b>0.65</b>	1.07
LinearSVR	0.31	0.34	0.37	<b>0.09</b>	0.91	<b>0.62</b>	<b>0.54</b>	0.91

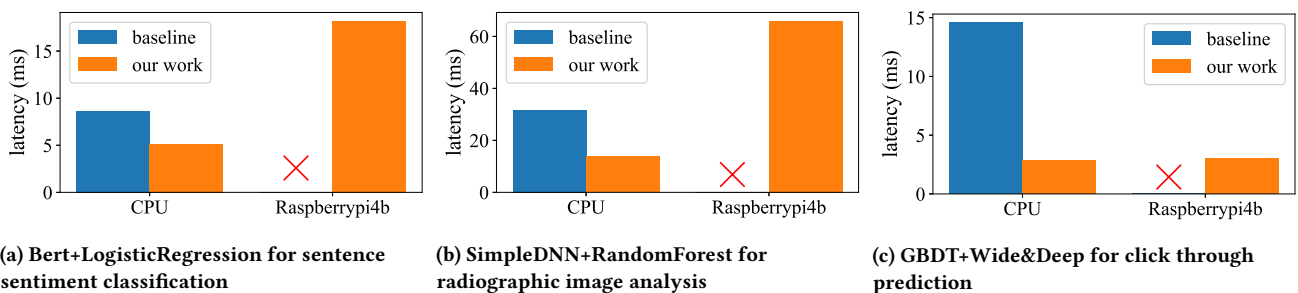


**Figure 8: The latency of a single query for CML and DL mixed pipelines. All three baselines cannot run on IoT devices.**

simple DNN to make feature engineering and CML models such as random forests to make a classification. We use CheXpert [21] as the dataset. The baseline implements DNN in PyTorch and random forest in sklearn. The result is shown in Fig. 8b. Our work achieves a 2.3x speedup on server CPUs. The pre-trained random forest cannot run on IoT devices, while our work solves this problem through cross-compilation.

**5.4.3 Click Through Rate Prediction.** The third case is click-through rate prediction used in recommendation systems of our anonymous industry partners, using GBDT [15] to extract features and the Wide and Deep [9] models to make prediction. We use avazu<sup>1</sup> as the dataset. The baseline implements GBDT in sklearn and Wide and Deep in PyTorch. The result is shown in Fig. 8c. We achieve 3.04x speedup on the server CPUs. The GBDT model in the baseline cannot be executed on IoT devices, while our latency on IoT devices is only 5.06 ms.

## 6 RELATED WORK

CML frameworks and libraries can be divided into three categories. (1) General-purpose solution uses one framework to support various models. Scikit-learn [32] is the most widely used CML framework on GitHub [33]. Spark MLlib [29] is an extension to Spark [48]. H2O [17] uses MapReduce [11] to support both CML and DL. There are many other works, such as Shogun [41] and RapidMiner [19]. These frameworks only support CPU, suffering from severe performance and portability issues. (2) Specific-purpose solution focuses on one type of model. LibLinear [14] supports logistic regression and linear SVM. LibSVM [5] focuses on SVMs. These works are limited to CPUs. Some other works attempt to support various hardware devices. XGBoost [6] implements gradient boosting decision tree algorithm on CPUs and GPUs. Muhsen Owaida et al. [31] bring XGBoost to FPGAs. Toby Sharp [39] implements decision trees and forests on GPUs. These frameworks only support a narrowed variety of models and solve the problem of portability to a certain extent. (3) Extension based on DL attempts to utilize DL frameworks to support CML models. TF-DF [43] is a decision forest library based on TensorFlow but is limited to CPUs. It's implemented in an ad-hoc way, losing the portability of DL frameworks. Hummingbird [30] is a general-purpose solution based on PyTorch, adding support for GPUs. They utilize those abstractions in DL frameworks directly without digging into the features of CML, missing many optimization chances.

## 7 CONCLUSION

This paper presented the design and implementation of CMLCompiler, a unified compiler for classical Machine Learning (CML) inference. CMLCompiler proposed two unified abstractions: operator representations and extended computational graphs (ECGs). Operator representations convert CML operators into tensor formats, while an ECG organizes these converted operators in an optimization-friendly way. The CMLCompiler framework performs the conversion and graph optimization based on two unified abstractions, then outputs an optimized computational graph to deep learning compilers or frameworks. CMLCompiler also enables the

<sup>1</sup><https://www.kaggle.com/c/avazu-ctr-prediction>

hybrid deployment of CML and DL with a unified framework. Our implementations of CMLCompiler on top of TVM show the effectiveness and achieve up to 4.38x speedup on CPU, 3.31x speedup on GPU, and 5.09x speedup on IoT devices, compared to the state-of-the-art solutions – scikit-learn, intel sklearn, and hummingbird. Our support for CML and DL mixed pipelines achieves up to 3.04x speedup compared with cross-framework implementations.

## A PROOF

Here we prove that  $\text{argmax}$  in Fig. 3 returns the leaf node finally reaches.  $N_S$ ,  $N_I$ , and  $N_L$  refer to the number of samples, internal nodes, and leaf nodes, respectively.  $I$  refers to internal nodes, numbered in the order of Level Order Traversal.  $L$  refers to leaf nodes, numbered in the order of In-Order Traversal.  $X \in \{0, 1\}^{N_S \times N_I}$  is the result after comparison with  $W_2$ . Each row  $X_i \in \{0, 1\}^{N_I}$  refers to choices for one sample  $x$ , marked as  $\vec{x}$ .  $W_3 \in \{0, 1\}^{N_I \times N_L}$  can be regarded as a list of column vector  $\{\vec{L}_1, \vec{L}_2, \dots, \vec{L}_{N_L}\}$ .  $\vec{L}_i \in \{0, 1\}^{N_I}$  represents the relationship between leaf node  $L_i$  and all internal nodes. Then we should prove that  $\text{argmax}(\vec{x} \cdot \vec{L}_1, \vec{x} \cdot \vec{L}_2, \dots, \vec{x} \cdot \vec{L}_{N_L})$  returns the leaf  $x$  reaches, where  $\text{argmax}$  returns the index of the maximum values among the input tensor. It returns the first index if maximum appears more than once. We assume that  $L_k$  is the leaf node  $x$  reaches.

First we prove that  $\vec{x} \cdot \vec{L}_k$  is the maximum value in  $\{\vec{x} \cdot \vec{L}_1, \vec{x} \cdot \vec{L}_2, \dots, \vec{x} \cdot \vec{L}_{N_L}\}$ . We define the path from root node  $I_0$  to  $L_k$  as the decision path of  $x$ .

$$L_k[i] = \begin{cases} 0, & \text{choose left in } I_i \text{ and } I_i \in \text{decisionpath} \\ 1, & \text{otherwise} \end{cases}$$

$$x[i] = \begin{cases} 0, & \text{choose left in } I_i \\ 1, & \text{choose right in } I_i \end{cases}$$

Because  $x$  reaches  $L_k$ , if  $x[i] = 1$  and  $I_i \in \text{decision path}$ , then  $L_k[i] = 1$ . DP represents decision path, right means choosing right in internal node and left means choosing left in internal node.

$$\begin{aligned} \vec{x} \cdot \vec{L}_k &= \sum_i x[i] * L_k[i] \\ &= \sum_{i, \text{right in } I_i} 1 * L_k[i] + \sum_{i, \text{left in } I_i} 0 * L_k[i] \\ &= \sum_{i, \text{right in } I_i} 1 * L_k[i] \\ &= \sum_{i, \text{right in } I_i \in \text{DP}} 1 * L_k[i] + \sum_{i, \text{right in } I_i \notin \text{DP}} 1 * L_k[i] \\ &= \sum_{i, \text{right in } I_i \in \text{DP}} 1 * 1 + \sum_{i, \text{right in } I_i \notin \text{DP}} 1 * 1 \\ &= \text{Counts of 1 in } \vec{x} \end{aligned}$$

$\vec{x}$  and  $\{\vec{L}_1, \vec{L}_2, \dots, \vec{L}_{N_L}\}$  are all 0-1 vector. Counts of 1 in  $\vec{x}$  is the maximum value of  $\{\vec{x} \cdot \vec{L}_1, \vec{x} \cdot \vec{L}_2, \dots, \vec{x} \cdot \vec{L}_{N_L}\}$ .

Then we prove that  $k$  is the first index that returns the maximum. We assume that there exists a leaf node  $L_t$  ahead of  $L_K$  which meets the condition  $\vec{x} \cdot \vec{L}_t == \text{maximum}$ . Now that  $L_t$  is ahead of  $L_k$  and the leaf nodes are numbered in a In-Order Traversal.  $\exists$  an internal node  $I_i$  where  $L_t$  is in the left subtree of  $I_i$  and  $L_k$  in the right subtree of  $I_i$ .  $X$  passes by  $I_i$  and reaches  $L_K$  in its right subtree, so  $x[i] = 1$ .  $L_t$  is in the left subtree of  $I_i$ , so  $L_t[i] = 0$ , where  $x[i]$  is multiplied

by zero. So  $\vec{x} \cdot \vec{L}_t < \text{maximum}$ . Conflict with the assumption that  $\vec{x} \cdot \vec{L}_t == \text{maximum}$ . So  $L_k$  is the first index that returns maximum.

## REFERENCES

- [1] Martin Abadi, Paul Barham, Jianmin Chen, Zhifeng Chen, Andy Davis, Jeffrey Dean, Matthieu Devin, Sanjay Ghemawat, Geoffrey Irving, Michael Isard, Manjunath Kudlur, Josh Levenberg, Rajat Monga, Sherry Moore, Derek G. Murray, Benoit Steiner, Paul Tucker, Vijay Vasudevan, Pete Warden, Martin Wicke, Yuan Yu, and Xiaoqiang Zheng. Tensorflow: A system for large-scale machine learning. In *Proceedings of the 12th USENIX Conference on Operating Systems Design and Implementation*, OSDI'16, page 265–283, USA, 2016. USENIX Association.
- [2] Amazon. The total cost of ownership (tco) of amazon sagemaker. [https://pages.awscloud.com/rs/112-TZM-766/images/Amazon\\_SageMaker\\_TCO\\_wf.pdf](https://pages.awscloud.com/rs/112-TZM-766/images/Amazon_SageMaker_TCO_wf.pdf), 2020.
- [3] Prajwal Bhargava, Aleksander Drozd, and Anna Rogers. Generalization in nli: Ways (not) to go beyond simple heuristics, 2021.
- [4] Leo Breiman. Random forests. *Machine learning*, 45(1):5–32, 2001.
- [5] Chih-Chung Chang and Chih-Jen Lin. Libsvm: a library for support vector machines. *ACM transactions on intelligent systems and technology (TIST)*, 2(3):1–27, 2011.
- [6] Tianqi Chen and Carlos Guestrin. Xgboost: A scalable tree boosting system. In *Proceedings of the 22nd ACM SIGKDD international conference on knowledge discovery and data mining*, pages 785–794, 2016.
- [7] Tianqi Chen, Thierry Moreau, Ziheng Jiang, Lianmin Zheng, Eddie Yan, Meghan Cowan, Haichen Shen, Leyuan Wang, Yuwei Hu, Luis Ceze, Carlos Guestrin, and Arvind Krishnamurthy. Tvm: An automated end-to-end optimizing compiler for deep learning. In *Proceedings of the 13th USENIX Conference on Operating Systems Design and Implementation*, OSDI'18, page 579–594, USA, 2018. USENIX Association.
- [8] Tianqi Chen, Lianmin Zheng, Eddie Yan, Ziheng Jiang, Thierry Moreau, Luis Ceze, Carlos Guestrin, and Arvind Krishnamurthy. Learning to optimize tensor programs. *Advances in Neural Information Processing Systems*, 31, 2018.
- [9] Heng-Tze Cheng, Levent Koc, Jeremiah Harmsen, Tal Shaked, Tushar Chandra, Hrishi Aradhye, Glen Anderson, Greg Corrado, Wei Choi, Mustafa Ispir, et al. Wide & deep learning for recommender systems. In *Proceedings of the 1st workshop on deep learning for recommender systems*, pages 7–10, 2016.
- [10] Scott Cyphers, Arjun K. Bansal, Anahita Bhiwandiwalla, Jayaram Bobba, Matthew Brookhart, Avijit Chakraborty, William Constable, Christian Convey, Leona Cook, Omar Kanawi, Robert Kimball, Jason Knight, Nikolay Korovaiko, Varun Kumar Vijay, Yixing Lao, Christopher R. Lishka, Jaikrishnan Menon, Jennifer Myers, Sandeep Aswath Narayana, Adam Procter, and Tristan J. Webb. Intel ngraph: An intermediate representation, compiler, and executor for deep learning. *CoRR*, abs/1801.08058, 2018.
- [11] Jeffrey Dean and Sanjay Ghemawat. Mapreduce: simplified data processing on large clusters. *Communications of the ACM*, 51(1):107–113, 2008.
- [12] Dheeru Dua and Casey Graff. UCI machine learning repository, 2017.
- [13] EasonLiao. Cudatree. <https://github.com/EasonLiao/CudaTree>, 2022.
- [14] Rong-En Fan, Kai-Wei Chang, Cho-Jui Hsieh, Xiang-Rui Wang, and Chih-Jen Lin. Liblinear: A library for large linear classification. *the Journal of machine Learning research*, 9:1871–1874, 2008.
- [15] Jerome H Friedman. Greedy function approximation: a gradient boosting machine. *Annals of statistics*, pages 1189–1232, 2001.
- [16] Ian Goodfellow, Jean Pouget-Abadie, Mehdi Mirza, Bing Xu, David Warde-Farley, Sherjil Ozair, Aaron Courville, and Yoshua Bengio. Generative adversarial nets. *Advances in neural information processing systems*, 27, 2014.
- [17] H2o.ai. H2o: Scalable machine learning platform. <https://github.com/h2oai/h2o-3>, 2022.
- [18] Kim Hazelwood, Sarah Bird, David Brooks, Soumith Chintala, Utku Diril, Dmytro Dzhulgakov, Mohamed Fawzy, Bill Jia, Yangqing Jia, Aditya Kalro, James Law, Kevin Lee, Jason Lu, Pieter Noordhuis, Misha Sulyanskiy, Liang Xiong, and Xiaodong Wang. Applied machine learning at facebook: A datacenter infrastructure perspective. In *2018 IEEE International Symposium on High Performance Computer Architecture (HPCA)*, pages 620–629, 2018.
- [19] Markus Hofmann and Ralf Klinkenberg. *RapidMiner: Data mining use cases and business analytics applications*. CRC Press, 2016.
- [20] Intel. Intel® extension for scikit-learn\*. <https://intel.github.io/scikit-learn-intelex/>, 2022.
- [21] Jeremy Irvin, Pranav Rajpurkar, Michael Ko, Yifan Yu, Silviana Ciurea-Ilcus, Chris Chute, Henrik Marklund, Behzad Haghgoo, Robyn Ball, Katie Shpanskaya, et al. CheXpert: A large chest radiograph dataset with uncertainty labels and expert comparison. In *Proceedings of the AAAI conference on artificial intelligence*, volume 33, pages 590–597, 2019.
- [22] Zhihao Jia, Oded Padon, James Thomas, Todd Warszawski, Matei Zaharia, and Alex Aiken. Taso: optimizing deep learning computation with automatic generation of graph substitutions. In *Proceedings of the 27th ACM Symposium on Operating Systems Principles*, pages 47–62, 2019.
- [23] Chris Lattner, Mehdi Amini, Uday Bondhugula, Albert Cohen, Andy Davis, Jacques Pienaar, River Riddle, Tatiana Shpeisman, Nicolas Vasilache, and Oleksandr Zinenko. Mlir: A compiler infrastructure for the end of moore's law. *arXiv preprint arXiv:2002.11054*, 2020.
- [24] Zewen Li, Fan Liu, Wenjie Yang, Shouheng Peng, and Jun Zhou. A survey of convolutional neural networks: analysis, applications, and prospects. *IEEE Transactions on Neural Networks and Learning Systems*, 2021.
- [25] Xiaoliang Ling, Weiwei Deng, Chen Gu, Hucheng Zhou, Cui Li, and Feng Sun. Model ensemble for click prediction in bing search ads. In *Proceedings of the 26th international conference on world wide web companion*, pages 689–698, 2017.
- [26] Wei-Yin Loh. Classification and regression trees. *Wiley interdisciplinary reviews: data mining and knowledge discovery*, 1(1):14–23, 2011.
- [27] Xiaofei Ma, Zhiguo Wang, Patrick Ng, Ramesh Nallapati, and Bing Xiang. Universal text representation from bert: An empirical study. *arXiv preprint arXiv:1910.07973*, 2019.
- [28] Larry Medsker and Lakhmi C Jain. *Recurrent neural networks: design and applications*. CRC press, 1999.
- [29] Xiangrui Meng, Joseph Bradley, Burak Yavuz, Evan Sparks, Shivaram Venkataraman, Davies Liu, Jeremy Freeman, DB Tsai, Manish Amde, Sean Owen, Doris Xin, Reynold Xin, Michael J. Franklin, Reza Zadeh, Matei Zaharia, and Ameet Talwalkar. Mllib: Machine learning in apache spark. *J. Mach. Learn. Res.*, 17(1):1235–1241, jan 2016.
- [30] Supun Nakandala, Karla Saur, Gyeong-In Yu, Konstantinos Karanasos, Carlo Curino, Markus Weimer, and Matteo Interlandi. A tensor compiler for unified machine learning prediction serving. In *14th {USENIX} Symposium on Operating Systems Design and Implementation ({OSDI} 20)*, pages 899–917, 2020.
- [31] Muhsen Owaida, Hantian Zhang, Ce Zhang, and Gustavo Alonso. Scalable inference of decision tree ensembles: Flexible design for cpu-fpga platforms. In *2017 27th International Conference on Field Programmable Logic and Applications (FPL)*, pages 1–8. IEEE, 2017.
- [32] Fabian Pedregosa, Gaël Varoquaux, Alexandre Gramfort, Vincent Michel, Bertrand Thirion, Olivier Grisel, Mathieu Blondel, Peter Prettenhofer, Ron Weiss, Vincent Dubourg, Jake Vanderplas, Alexandre Passos, David Cournapeau, Matthieu Brucher, Matthieu Perrot, and Édouard Duchesnay. Scikit-learn: Machine learning in python. *J. Mach. Learn. Res.*, 12(null):2825–2830, nov 2011.
- [33] Fotis Psallidas, Yiwen Zhu, Bojan Karlas, Matteo Interlandi, Avrilis Floratou, Konstantinos Karanasos, Wentao Wu, Ce Zhang, Subru Krishnan, Carlo Curino, and Markus Weimer. Data science through the looking glass and what we found there. *CoRR*, abs/1912.09536, 2019.
- [34] Sushmita Ray. A quick review of machine learning algorithms. In *2019 International conference on machine learning, big data, cloud and parallel computing (COMITCon)*, pages 35–39. IEEE, 2019.
- [35] James Reed, Zachary DeVito, Horace He, Ansley Ussery, and Jason Ansel. torch. fx: Practical program capture and transformation for deep learning in python. *Proceedings of Machine Learning and Systems*, 4:638–651, 2022.
- [36] Nils Reimers and Iryna Gurevych. Sentence-bert: Sentence embeddings using siamese bert-networks. *arXiv preprint arXiv:1908.10084*, 2019.
- [37] Shayle R Searle and Marvin HJ Gruber. *Linear models*. John Wiley & Sons, 2016.
- [38] Duhita Sengupta, Sk Nishan Ali, Aditya Bhattacharya, Joy Mustafi, Asima Mukhopadhyay, and Kaushik Sengupta. Nuclear morphology optimized deep hybrid learning (numodril): A novel architecture for accurate diagnosis/prognosis of ovarian cancer. *bioRxiv*, 2020.
- [39] Toby Sharp. Implementing decision trees and forests on a gpu. In *European conference on computer vision*, pages 595–608. Springer, 2008.
- [40] Richard Socher, Alex Perelygin, Jean Wu, Jason Chuang, Christopher Manning, Andrew Ng, and Christopher Potts. Parsing With Compositional Vector Grammars. In *EMNLP*, 2013.
- [41] Søren Sonnenburg, Gunnar Rätsch, Sebastian Henschel, Christian Widmer, Jonas Behr, Alexander Zien, Fabio de Bona, Alexander Binder, Christian Gehl, and Vojtěch Franc. The shogun machine learning toolbox. *The Journal of Machine Learning Research*, 11:1799–1802, 2010.
- [42] Shan Suthaharan. Support vector machine. In *Machine learning models and algorithms for big data classification*, pages 207–235. Springer, 2016.
- [43] TensorFlow. Tensorflow decision forests. [https://www.tensorflow.org/decision\\_forests](https://www.tensorflow.org/decision_forests), 2022.
- [44] Jake VanderPlas. *Python data science handbook: Essential tools for working with data*. " O'Reilly Media, Inc.", 2016.
- [45] Thomas Wolf, Lysandre Debut, Victor Sanh, Julien Chaumond, Clement Delangue, Anthony Moi, Pierrick Cistac, Tim Rault, Rémi Louf, Morgan Funtowicz, Joe Davison, Sam Shleifer, Patrick von Platen, Clara Ma, Yacine Jernite, Julien Plu, Canwen Xu, Teven Le Scao, Sylvain Gugger, Mariama Drame, Quentin Lhoest, and Alexander M. Rush. Transformers: State-of-the-art natural language processing. In *Proceedings of the 2020 Conference on Empirical Methods in Natural Language Processing: System Demonstrations*, pages 38–45, Online, October 2020. Association for Computational Linguistics.
- [46] Carole-Jean Wu, David Brooks, Kevin Chen, Douglas Chen, Sy Choudhury, Marat Dukhan, Kim Hazelwood, Eldad Isaac, Yangqing Jia, Bill Jia, Tommer Leyvand,

Hao Lu, Yang Lu, Lin Qiao, Brandon Reagen, Joe Spisak, Fei Sun, Andrew Tulloch, Peter Vajda, Xiaodong Wang, Yanghan Wang, Bram Wasti, Yiming Wu, Ran Xian, Sungjoo Yoo, and Peizhao Zhang. Machine learning at facebook: Understanding inference at the edge. In *2019 IEEE International Symposium on High Performance Computer Architecture (HPCA)*, pages 331–344, 2019.

[47] Doris Xin, Hui Miao, Aditya Parameswaran, and Neoklis Polyzotis. Production machine learning pipelines: Empirical analysis and optimization opportunities. In *Proceedings of the 2021 International Conference on Management of Data*, pages 2639–2652, 2021.

[48] Matei Zaharia, Mosharaf Chowdhury, Michael J Franklin, Scott Shenker, and Ion Stoica. Spark: cluster computing with working sets. In *Proceedings of the 2nd USENIX conference on Hot topics in cloud computing*, 2010.

[49] Lianmin Zheng, Chengfan Jia, Minmin Sun, Zhao Wu, Cody Hao Yu, Ameer Haj-Ali, Yida Wang, Jun Yang, Danyang Zhuo, Koushik Sen, Joseph E. Gonzalez, and Ion Stoica. *Anso: Generating High-Performance Tensor Programs for Deep Learning*. USENIX Association, USA, 2020.